JOURNAL OF THERMOPHYSICS AND HEAT TRANSFER
Vol. 12, No. 2, April–June 1998

Shape Identification Problem in Estimating Geometry of Multiple Cavities

Cheng-Hung Huang* and Cheng-Chia Chiang†
National Cheng Kung University, Tainan 70101, Taiwan, Republic of China
and
Hsi-Mei Chen‡
Kung Shan Institute of Technology, Tainan Hsien 70401, Taiwan, Republic of China

A shape identification problem (or an inverse geometry heat conduction problem) is solved to detect the unknown shape of multiple cavities by using the steepest descent method (SDM). One of the advantages of using the SDM lies in that it easily can handle problems having a large number of unknown parameters. The boundary element method is used to calculate the direct as well as the sensitivity and adjoint problems because of its characteristic of easily handling the problem considered here. Results obtained by using the SDM to solve the inverse problems are verified based on the numerical experiments. One concludes that the SDM is applied successfully in estimating the arbitrary shape of cavities, and the rate of convergence is also very fast. Moreover, the accuracy of the inverse solutions depends on the positions of the sensors. When the sensors are arranged closer to the cavities, the estimated results are more accurate. Finally, the effects of the measurement errors on the inverse solutions are discussed.

Nomenclature

$f(x, y)$	=	unknown irregular cavities configuration
G, H	=	geometry-dependent matrix
J	=	functional, Eq. (5)
J'	=	gradient of functional, Eq. (14)
q	=	heat flux density
$T(x, y)$	=	estimated dimensionless temperature
$Y(x, y)$	=	measured temperature
β	=	search step size
Γ	=	boundary of the computational domain
$\Delta T(x, y)$	=	sensitivity function, Eq. (7)
$\delta(\ )$	=	Dirac delta function
ε	=	convergence criteria
$\lambda(x, y)$	=	Lagrange multiplier defined by equation (12)
σ	=	standard deviation of the measurement errors
Ω	=	computational domain
ω	=	random number

Superscripts

n	=	iteration index
$\hat{}$	=	estimated values
$*$	=	fundamental solution

I. Introduction

TRADITIONAL inverse heat conduction problems, such as the determination of boundary conditions,[1] thermal properties,[2] heat generation,[3] contact resistance,[4] etc., can be found in several engineering fields. Recently, inverse geometry problems (shape identification problems) have become another area of active research, and many researchers have used infrared scanners in their applications to nondestructive evaluation (NDE).

Hsieh and Su[5] used pattern recognition techniques and analytical methods to detect regularly shaped subsurface cavity walls included in regular bounded domains. Hsieh and Kassab[6] successfully detected a cavity with irregularly shaped walls contained within a bounding body whose walls are restricted to be parallel to a separable coordinate system. Kassab and Hsieh[7] detected the back-surface position in a corner region. Hsieh et al.[8] coupled the boundary-element method with the inverse problem in cavity estimation. More recently, Kassab and Pollard[9] used a cubic spline anchored grid pattern (AGP) algorithm in estimating the irregular cavity. In Ref. 9 only a very few elements were used to describe the unknown cavity because the technique they used belongs to parameter estimation,[10] i.e., a small number of unknown parameters are to be estimated. However, one should note that for a cavity with a very complicated shape, the number of elements used should be increased; otherwise accurate solutions cannot be obtained.

The preceding reviewed literature indicates that the techniques used belong to the parameter estimation[10]; therefore, when the number of unknown parameters is increased tremendously (such as in the problem of estimating very complicated shapes of the cavities or in the unsteady-state problem), the algorithm may converge very slowly or even may not work. For example, in Ref. 9, as the unknown parameters are increased, the CPU time needed for constructing the Jacobian matrix will also be increased and, therefore, will slow the rate of convergence. This phenomenon has been discussed by Huang and Chao,[11] and they concluded that the techniques of function estimation will be much better than parameter estimation, because the number of unknown parameters are unlimited when using the technique of function estimation. The present paper is actually the extended work of Ref. 11, where the search directions are restricted in the y direction, i.e., the unknown parameters are y coordinates only. However, for the present study, we do not confine the search directions, i.e., the unknown parameters become x and y coordinates.

In this paper the steepest descent method (SDM) for the numerical solution to the inverse geometry problem of identifying the unknown irregular-shaped cavities from temperature measurements, based on the boundary element method (BEM), is considered. Such identification problems can be stated in various contexts: acoustics, elastodynamics, and ther-

Received July 10, 1997; revision received Nov. 18, 1997; accepted for publication Dec. 4, 1997.

*Professor, Department of Naval Architecture and Marine Engineering.

†Graduate Student, Department of Naval Architecture and Marine Engineering.

‡Lecturer, Department of Information Management.

mal sciences, and can lead to applications to NDE techniques and other identification problems.

The use of the BEM is suggested by the basic nature of the inverse problem (to search an unknown domain, thus an unknown surface) because domain discretization is avoided. More specifically, the advantages gained by a BEM-based algorithm are the ability to readily accommodate the changes in the unknown boundary shape as it evolves from its initial to its final shape and the ability to handle the problem of multiple internal boundaries.

The present work addresses the developments of the steepest descent algorithm for estimating unknown cavity shapes. The steepest descent method derives from the perturbation principle and transforms the inverse problem to the solution of three problems, namely, the direct problem, the sensitivity problem, and the adjoint problem. This method will be discussed in detail in the following text.

II. Direct Problem

To illustrate the methodology for developing expressions for use in determining an unknown cavity geometry in a homogeneous medium, we consider the following two-dimensional, steady-state, inverse heat conduction problem. For a domain Ω, the boundary conditions along boundaries Γ_i, $i = 1$–4, are subjected to the prescribed temperature conditions, T_1, T_2, T_3, and T_4, respectively. The boundary Γ_5 along the unknown cavity is also subject to a known temperature distribution T_5. Figure 1 shows the geometry and coordinates for the two-dimensional physical problem considered here, where the solid dots denote the sensor locations. The mathematical formulation of this steady-state heat conduction problem in dimensionless form is given by

$$\frac{\partial^2 T}{\partial^2 x} + \frac{\partial^2 T}{\partial^2 y} = 0 \quad \text{in} \quad \Omega \tag{1a}$$

$$T = T_i \quad \text{along} \quad \Gamma_i, \qquad i = 1\text{–}4 \tag{1b}$$

$$T = T_5 \quad \text{along} \quad \Gamma_5 \equiv f(x, y) \tag{1c}$$

The preceding problem is solved by the following BEM algorithm.

For a constant property, steady-state heat-conduction problem with a domain Ω and boundary Γ, the boundary integral equation for this problem without generation term can be derived as[12]

$$cT_m + \int_\Gamma Tq^* \, d\Gamma = \int_\Gamma qT^* \tag{2}$$

where m = point on Γ or in Ω, $c = 1$ if m is in Ω, $c < 1$ if m is on Γ ($c = 0.5$ if Γ is smooth at m), T^* = stationary fundamental solution, and q^* = normal derivative of T^*. Therefore, $T^* = 1/2\pi \ln(1/r)$ in two dimensions where r = distance from m to a point of Γ.[12]

Generally speaking, the discretization of Γ into k boundary elements allows substitution into the boundary integral Eq. (2), expressed for each boundary element of the algebraic linear system

$$\boldsymbol{CT} + \boldsymbol{HT} = \boldsymbol{Gq} \tag{3}$$

where $\boldsymbol{T}$ is the vector of temperature boundary elements, $\boldsymbol{q}$ is the vector of boundary heat flux densities, H and G are the geometry dependent matrices, and C is the diagonal matrix.

Once all unknowns are passed to the left-hand side and the knowns are gathered on the right-hand side (RHS), one can write

$$\boldsymbol{AX} = \boldsymbol{B} \tag{4}$$

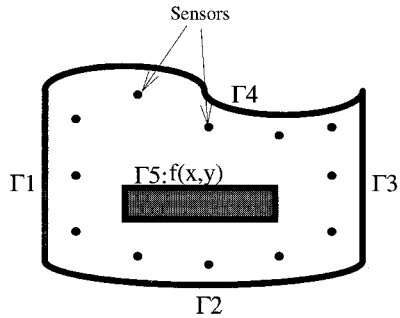

Fig. 1 System under consideration.

where $\boldsymbol{X}$ is the vector of unknown T and q on the boundary. $\boldsymbol{B}$ is found by multiplying the corresponding columns by the known values of T or q.

The computer program for the preceding problem is modified based on the textbook by Brebbia and Dominguez,[12] and linear boundary elements are adopted for all the examples illustrated here.

The direct problem considered here is concerned with the determination of the medium temperature when the cavity geometry $f(x, y)$ and the boundary conditions at all boundaries are known.

III. Inverse Problem

For the inverse problem, the cavity geometry $f(x, y)$ is regarded as being unknown, but everything else in Eq. (1) is known. In addition, temperature readings taken at appropriate locations are considered available.

Referring to Fig. 1, we assume that M sensors installed internal to the domain are used to record the temperature information to identify the cavity configuration $f(x, y)$ in the inverse calculations. Let the temperature reading taken within these sensors be denoted by $Y(x_i, y_i) \equiv Y_i$, $i = 1$ to M, where M represents the number of thermocouples. We note that the measured temperatures Y_i contain measurement errors. Then the inverse problem can be stated as follows: by utilizing the previously mentioned measured temperature data Y_i, estimate the unknown shape $f(x, y)$ of the cavity.

The solution of the present inverse problem is to be obtained in such a way that the following functional is minimized:

$$J[f(x, y)] = \sum_{i=1}^{M} [T_i - Y_i]^2 \tag{5}$$

where T_i are the estimated or computed temperatures at the measurement locations (x_i, y_i). These quantities are determined from the solution of the direct problem given previously by using an estimated $\hat{f}(x, y)$ for the exact $f(x, y)$.

IV. Steepest Descent Method for Minimization

The steepest descent method is similar to but simpler than the conjugate gradient method,[13] because the calculation of the conjugate coefficient and direction of descent is not needed. We find that it can achieve our goal in the present inverse study, and it converges very fast. The following iterative process based on the steepest descent method is now used for the estimation of the unknown boundary function $f(x, y)$ by minimizing the functional $J[f(x, y)]$:

$$\hat{f}^{n+1} = \hat{f}^n - \beta^n J'^n \tag{6a}$$

or more explicitly

$$\hat{x}^{n+1} = \hat{x}^n - \beta^n J'^n(x, y) \times \cos\theta \tag{6b}$$

$$\hat{y}^{n+1} = \hat{y}^n - \beta^n J'^n(x, y) \times \sin\theta \tag{6c}$$

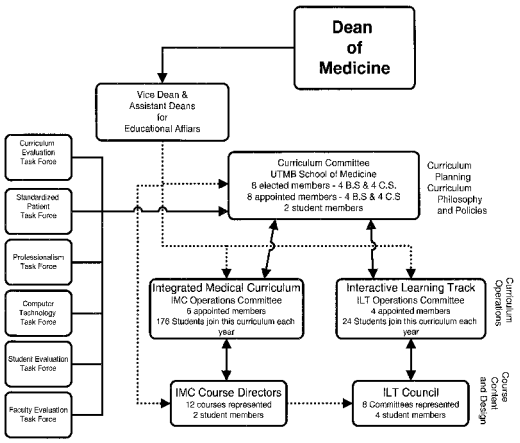

Fig. 2 Graphical analysis of SDM from n to $(n\ 1\ 1)$ iterations.

$$\hat{f}^{n+1}(x, y) = f(\hat{x}^{n+1}, \hat{y}^{n+1}) \tag{6d}$$

where θ is the angle between horizontal and normal outward direction of the unknown boundary as shown in Fig. 2. The value of θ can be calculated for any given configuration. β^n is the search step size in going from iteration n to iteration $n + 1$, and $J'^n(x, y)$ is the gradient in the outward normal direction.

To perform the iterations according to Eqs. (6a–6d), we need to compute the step size β^n and the gradient of the functional $J'^n(x, y)$. To develop expressions for the determination of these two quantities, a sensitivity problem and an adjoint problem are constructed as described next.

V. Sensitivity Problem and Search Step Size

The sensitivity problem is obtained in the following manner from the original direct problem defined by Eq. (1). It is assumed that when $f(x, y)$ undergoes a variation $\Delta f(x, y)$, $T(x, y)$ is perturbed by $T + \Delta T$. Then replacing in the direct problem f with $f + \Delta f$ and T with $T + \Delta T$, subtracting from the resulting expressions the direct problem, and neglecting the second-order terms, the following sensitivity problems for the sensitivity function ΔT are obtained:

$$\frac{\partial^2 \Delta T}{\partial x^2} + \frac{\partial^2 \Delta T}{\partial y^2} = 0 \quad \text{in} \quad \Omega \tag{7a}$$

$$\Delta T = 0 \quad \text{along} \quad \Gamma_1, \Gamma_2, \Gamma_3, \Gamma_4 \tag{7b}$$

$$\Delta T = \Delta f \frac{\partial T}{\partial n} \quad \text{along} \quad \Gamma_5 \tag{7c}$$

where $\partial T/\partial n$ represents the temperature gradient along the normal direction of Γ_5. The BEM technique is used to solve this sensitivity problem.

The functional $J(\hat{f}^{m+1})$ for iteration $n + 1$ is obtained by rewriting Eq. (5) as

$$J[\hat{f}^{n+1}] = \sum_{i=1}^{M} [T_i(\hat{f}^n - \beta^n J'^m) - Y_i]^2 \tag{8a}$$

where we replaced $\hat{f}^{n+1}$ by the expression given by Eq. (6a). If temperature $T_i(\hat{f}^n - \beta^n J'^n)$ is linearized by a Taylor expansion, Eq. (8a) takes the form

$$J(\hat{f}^{n+1}) = \sum_{i=1}^{M} [T_i(\hat{f}^n) - \beta^n \Delta T_i(J'^n) - Y_i]^2 \tag{8b}$$

where $T_i(\hat{f}^n)$ is the solution of the direct problem at (x_i, y_i) by using estimate $\hat{f}^n(x, y)$ for exact $f(x, y)$. The sensitivity functions $\Delta T_i(J'^n)$ are taken as the solutions of problem (7) at the measured positions at (x_i, y_i) by letting $\Delta f = J'^n$. The search step size β^n is determined by minimizing the functional given by Eq. (8b) with respect to β^n. The following expression results:

$$\beta^n = \sum_{i=1}^{M} (T_i - Y_i)\Delta T_i \Big/ \sum_{i=1}^{M} (\Delta T_i)^2 \tag{9}$$

VI. Adjoint Problem and Gradient Equation

To obtain the adjoint problem, Eq. (1a) is multiplied by the Lagrange multiplier (or adjoint function) $\lambda(x, y)$ and the resulting expression is integrated over the correspondent space domains. Then the result is added to the RHS of Eq. (5) to yield the following expression for the functional $J[f(x, y)]$:

$$J[f(x, y)] = \sum_{i=1}^{M} [T_i - Y_i]^2 + \int_\Omega \lambda \left(\frac{\partial^2 T}{\partial x^2} + \frac{\partial^2 T}{\partial y^2} \right) d\Omega \tag{10}$$

The variation ΔJ is obtained by perturbing f by Δf and T by ΔT in Eq. (1), subtracting from the resulting expression the original Eq. (1), and neglecting the second-order terms. We thus find

$$\Delta J = \int_\Omega 2(T - Y)\Delta T \delta(x - x_i)\delta(y - y_i)\, d\Omega + \int_\Omega \lambda \left(\frac{\partial^2 \Delta T}{\partial x^2} + \frac{\partial^2 \Delta T}{\partial y^2} \right) d\Omega \tag{11}$$

where $\delta(x - x_i)$ and $\delta(y - y_i)$ are the Dirac delta functions, and (x_i, y_i), $i = 1$ to M, refer to the measured positions. In Eq. (11), the second domain integral term is reformulated based on Green's second identity; the boundary conditions of the sensitivity problem given by Eqs. (7b) and (7c) are utilized and then ΔJ is allowed to go to zero. The vanishing of the integrands containing ΔT leads to the following adjoint problem for the determination of $\lambda(x, y)$:

$$\frac{\partial^2 \lambda}{\partial x^2} + \frac{\partial^2 \lambda}{\partial y^2} + 2(T - Y)\delta(x - x_i)\delta(y - y_i) = 0 \tag{12a}$$

$$\lambda = 0 \quad \text{along} \quad \Gamma_1, \Gamma_2, \ldots, \Gamma_5 \tag{12b}$$

The standard techniques of BEM can be used to solve the preceding adjoint problem. Finally, the following integral term remains:

$$\Delta J = \int_{\Gamma_5} - \left[\frac{\partial \lambda}{\partial n} \frac{\partial T}{\partial n} \right] \Delta f(x, y)\, d\Gamma \tag{13a}$$

From the definition in Ref. 13, the functional increment can be presented as

$$\Delta J = \int_{\Gamma_5} J'(x, y)\Delta f(x, y)\, d\Gamma \tag{13b}$$

A comparison of Eqs. (13a) and (13b) leads to the following expression for the gradient of functional $J'(x, y)$ of the functional $J[f(x, y)]$:

$$J'(x, y) = -\frac{\partial \lambda}{\partial n} \frac{\partial T}{\partial n}\bigg|_{\Gamma_5} \tag{14}$$

The calculation of the gradient equation is the most important part of the SDM because it plays a significant role in the inverse calculation.

VII. Stopping Criterion

If the problem contains no measurement errors, the traditional check condition specified as follows can be used as the stopping criteria:

$$J[f^{n+1}(x, y)] < \varepsilon \tag{15a}$$

where ε is a small specified number and the monotonic convergence can be obtained with the SDM. However, the observed temperature data may contain measurement errors. Therefore, we do not expect functional Eq. (5) to be equal to zero at the final iteration step. Following the experience of Ref. 13, we use the discrepancy principle as the stopping criterion, i.e., we assume that the temperature residuals may be approximated by

$$T_i - Y_i \approx \sigma \tag{15b}$$

where σ is assumed to be a constant.

Substituting Eq. (15b) into Eq. (5), the following expression is obtained for ε:

$$\varepsilon = M\sigma^2 \tag{15c}$$

Then the stopping criterion is given by Eq. (15a) with ε determined from Eq. (15c).

VIII. Computational Procedure

The computational procedure for the solution of this inverse problem using the conjugate gradient method may be summarized as follows:

Suppose $\hat{f}^n(x, y)$ is available at iteration n.

Step 1. Solve the direct problem given by Eq. (1) for $T(x, y)$.

Step 2. Examine the stopping criterion given by Eq. (15a) with ε given by Eq. (15c). Continue if not satisfied.

Step 3. Solve the adjoint problem given by Eq. (12) for $\lambda(x, y)$.

Step 4. Compute the gradient of the functional J' from Eq. (14).

Step 5. Set $\Delta f(x, y) = J'^n(x, y)$, and solve the sensitivity problem given by Eq. (7) for $\Delta T(x, y)$.

Step 6. Compute the search step size β^n from Eq. (9).

Step 7. Compute the new estimation for $\hat{f}^{n+1}(x, y)$ from Eq. (6c) and return to step 1.

IX. Results and Discussions

To illustrate the validity of the present inverse algorithm in identifying irregular configuration of cavities from the knowledge of temperature recordings, we consider three specific examples where the number of cavities internal to the domain is assumed to be one, two, and three, respectively.

The objective of this paper is to show the accuracy of the present approaches in estimating $f_j(x, y)$, $j = 1$ to J, and J is the number of cavities, with no prior information on the functional form of the unknown cavities, which is the so-called function estimation. Moreover, it can be shown numerically that the number of sensors can be reduced when the steepest descent method is applied.

To compare the results for situations involving random measurement errors, we assume normally distributed uncorrelated errors with zero mean and constant standard deviation. The simulated inexact measurement data $\boldsymbol{Y}$ can be expressed as

$$\boldsymbol{Y} = \boldsymbol{Y}_{\text{exact}} + \omega\sigma \tag{16}$$

where $\boldsymbol{Y}_{\text{exact}}$ is the solution of the direct problem with an exact $f_j(x, y)$, and ω is a random normal variable generated by subroutine DRNNOR of the International Mathematical and Statistical Library[14] and will be within -2.576–2.576 for a 99% confidence bounds.

The advantages of using the steepest descent method are that 1) it does not require a very accurate initial guess of the unknown shapes and 2) it can be extended easily to the transient problem where the unknown cavities are function of positions and time. We now present three numerical experiments in determining $f(x, y)$ by the inverse analysis.

A. Numerical Test Case 1: Single Cavity Estimation

The unknown configuration of the cavity is assumed to be a star-shape form as shown in Fig 3. The prescribed temperatures along Γ_1, Γ_2, Γ_3, and Γ_4 are 3, 6, 5, and 4, respectively, whereas the temperature along Γ_5 $[f_1(x, y)]$ is 20. The number of linear elements used for external and internal boundaries are both 40, which implies that the unknown parameters of x and y coordinates are 80 in the present case.

The inverse analysis is first performed by using 40 thermocouple measurements (referring to Fig. 3, where the symbol $\times$ denotes the sensor's location). When assuming exact measurements ($\sigma = 0.0$) and using a circle with center at (0,0) and radius $r = 1.5$ as the initial guess, the estimated shape of cavity by using the SDM is shown in Fig. 3 when 25 iterations are used. It can be seen from this figure that the scheme obtained good estimation of $f_1(x, y)$, and the CPU time (on a 586-60 MHz personal computer) used in the SDM is about 60 s.

Next, let us see what will happen when the sensors are moved closer to the unknown cavity. The computational situations are the same as for the previous problem except that the thermocouples are arranged as shown in Fig. 4. The inverse solution using 25 iterations is shown in Fig. 4. It is clear from Figs. 3 and 4 that the estimated shape of cavity $f_1(x, y)$ becomes more accurate when the sensors are arranged closer to it.

The preceding test cases seem unrealistic because too many sensors were used in the numerical experiments. Now the question arises, can the number of sensors be reduced with the present approach?

Here, for the SDM, the measurement temperatures at sensor locations represent the internal point heat sources that appeared

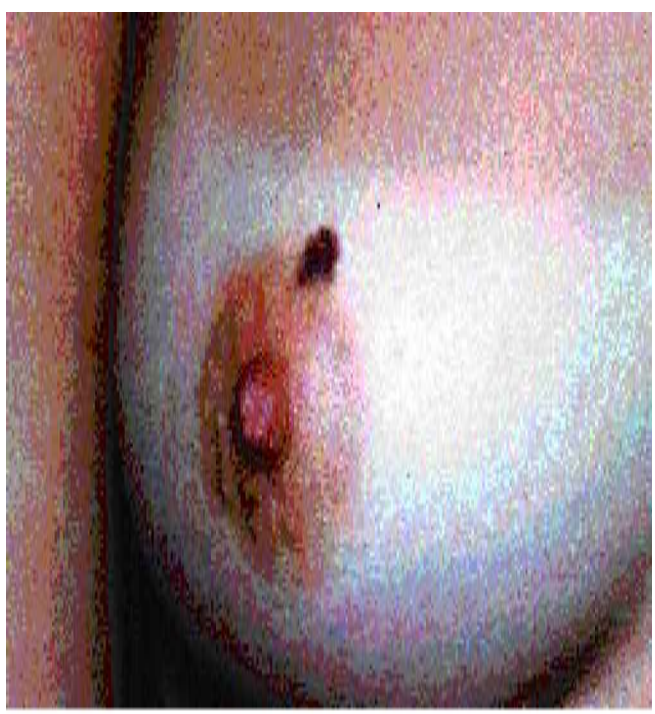

(A)

Fig. 3 Exact and estimated cavity with further measurements when using s = 0.0 and M = 40 in test case 1.

in adjoint Eq. (12a). It is possible to reduce the number of point heat sources even though it will influence the value of $J'(x, y)$. Now the question is, will this strategy influence the accuracy of the inverse solutions? To answer this, the numerical experiment proceeds to the next case, where the calculating conditions are the same as were used in Fig. 4, except that the number of sensors is now reduced to $M = 20$.

The inverse solutions in predicting $f(x, y)$ under such an assumption using the SDM are shown in Fig. 5. The comparison of Figs. 4 and 5 reveals that the reduction of the number of sensors does not make the inverse solutions worse, which means when the SDM is applied the number of sensors can be reduced.

However, when the number of sensors is further reduced to 10, the differences between exact and estimated cavities become large. This implies that the number of sensors needed depends on the required accuracy of inverse solutions, and this can be done in the numerical analysis before the installation of experimental sensors.

Now let us see the influence of the initial guess on the inverse solutions. The computational conditions are the same as used in Fig. 5, except that the initial guess of the cavity is now chosen as a circle with the center at $(-0.7,-0.7)$ and radius $r = 1.0$. The estimation of cavity under such an assumption is shown in Fig. 6. The comparison of Figs. 5 and 6 indicates that when different shapes and locations of the initial guesses are used, a consistent inverse solution can still be obtained.

Finally, the measurement errors will be considered. When the standard deviation of the measurement errors with $\sigma = 0.1$ and 0.2 are assumed, the simulated inexact measurement temperature can be obtained from Eq. (16). Here, $\sigma = 0.1$ and 0.2 represent about 1 and 2% measurement error, respectively, because the average measured temperature is about 10. In accordance with the discrepancy principle, the stopping criteria can be obtained from Eq. (15c) when the measurement errors are considered. The number of iterations needed for $\sigma = 0.1$ and 0.2 are 19 (45 s CPU time) and 11 (27 s CPU time), respectively. The estimated cavities for these two cases are shown in Figs. 7 and 8. From Figs. 6–8 we observe that, as the measurement errors are increased, the accuracy of the inverse solutions is decreased; however, they are still reliable. Therefore, the present technique provides a confident estimation.

(F)

Fig. 4 Exact and estimated cavity when using $s = 0.0$ and $M = 40$ in test case 1.

(G)

Fig. 5 Exact and estimated cavity when using $s = 0.0$ and $M = 20$ in test case 1.

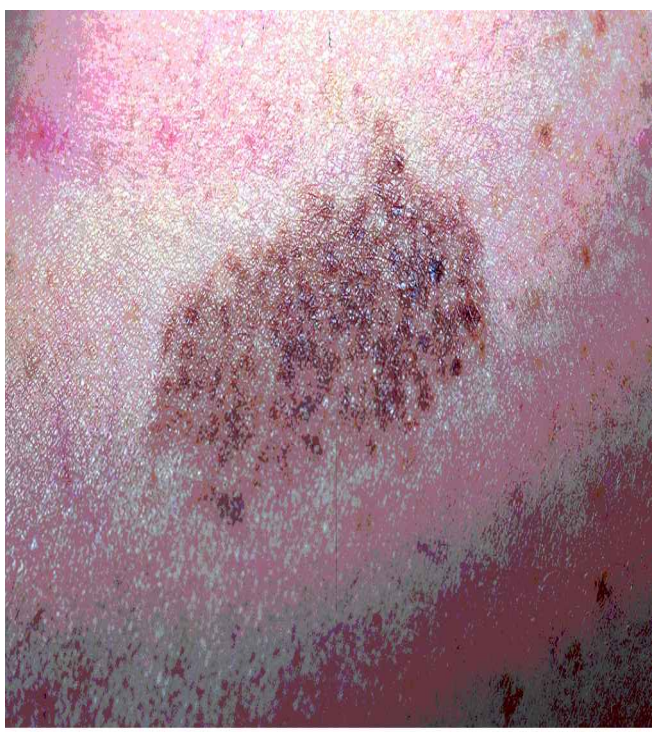

(A)

Fig. 6 Exact and estimated cavity when using $s = 0.0$, $M = 20$, and different initial guess in test case 1.

B. Numerical Test Case 2: Two-Cavity Estimation

To show the ability to handle multiple-cavity estimation, in the second test case we consider a domain with two unknown

(B)

Fig. 7 Exact and estimated cavity when using s = 0.1 and M = 20 in test case 1.

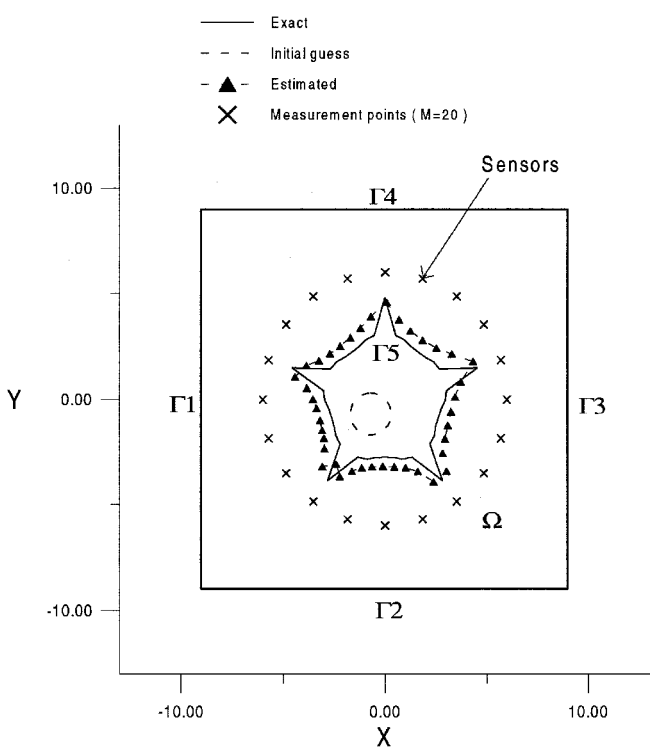

Fig. 8 Exact and estimated cavity when using s = 0.2 and M = 20 in test case 1.

internal cavities, i.e., a pentagon and a rectangular shape, as shown in Fig. 9. The prescribed temperatures along Γ_1, Γ_2, Γ_3, and Γ_4 are the same as used in numerical test case 1, while temperatures along Γ_5 [$f_1(x, y)$] and Γ_6[$f_2(x, y)$] are taken as 18 and 20, respectively. The number of linear elements used for the external boundary are 40, and for the internal boundaries they are both 20; therefore, the number of unknown parameters is the same as in case 1.

The inverse analysis is performed by using 40 thermocouple measurements arranged as shown in Fig. 9, where the symbol $\times$ denotes the sensor's location. When assuming exact measurements (σ = 0.0) and using two circles with radius r = 0.8 and centers at (−4.0, 2.8) and (4.0, −3.0) as the initial guesses, the estimated shape of cavities by using the SDM is shown in Fig. 9 using 15 iterations. It can be seen from this figure that the scheme obtains reliable estimations of $f_1(x, y)$ and $f_2(x, y)$, except for the center region, and the CPU time (on a 586-60 MHz personal computer) used in the SDM is about 32 s. The reason for inaccurate estimation near the center region of the domain is that there are no sensors installed within this region, thus no temperature readings can be obtained. The nature of the inverse problems lies in that good information should have been provided to obtain good estimation. When no sensors are placed in the positions between two cavities, good information cannot be obtained and, therefore, the estimations become inaccurate.

Next, when the standard deviation of the measurement errors with σ = 0.4 and 0.7 are assumed, the simulated inexact measurement temperature can be obtained from Eq. (16). Here, σ = 0.4 and 0.7 represent about 5 and 9% measurement error, respectively, because the average measured temperature is about 8. The inverse solution can be obtained after 3 (11 s CPU time) and 2 (8 s CPU time) iterations for σ = 0.4 and 0.7, respectively. The estimated cavities for these two cases are shown in Figs. 10 and 11. From Figs. 9–11, we conclude that as the measurement errors are increased, the SDM still produces confident inverse solutions.

C. Numerical Test Case 3: Three-Cavity Estimation

In the third test case we consider a domain with three unknown internal cavities, i.e., circular, rectangular, and triangular shapes as shown in Fig. 12. The prescribed temperature along Γ_1 is equal to 5, whereas the temperatures along Γ_2[$f_1(x, y)$], Γ_3[$f_2(x, y)$], and Γ_4[$f_3(x, y)$] are all taken to be 20. The number of linear elements used for the external boundary are 30, and for the internal circular, rectangular, and triangular boundaries they are 20, 20, and 15, respectively. Therefore, the unknown number of parameters of x and y coordinates is equal to 110 in test case 3.

Fig. 9 Exact and estimated cavities when using s = 0.0 and M = 40 in test case 2.

(B)

Fig. 10 Exact and estimated cavities when using s = 0.4 and M = 40 in test case 2.

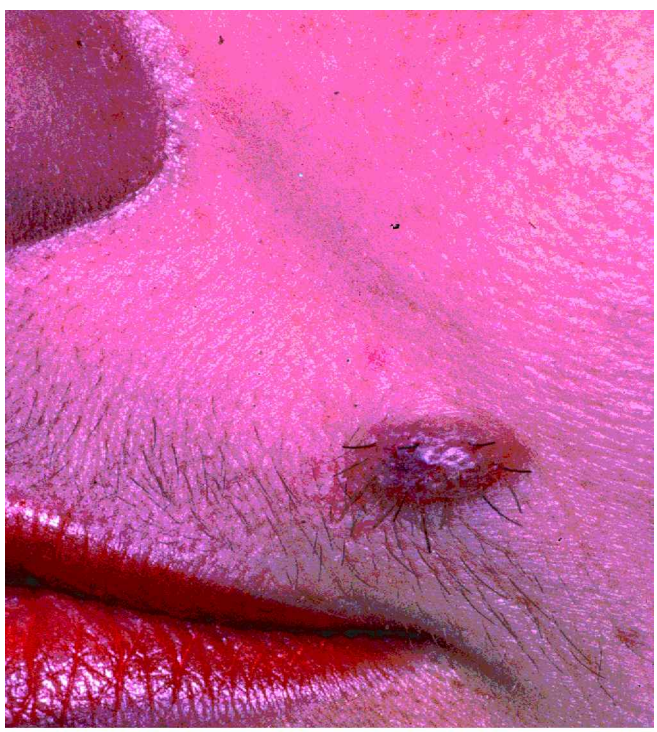

(C)

Fig. 11 Exact and estimated cavities when using s = 0.7 and M = 40 in test case 2.

The inverse analysis is performed using 40 thermocouple measurements arranged as shown in Fig. 12, where the symbol $\times$ denotes the sensor's location. When assuming exact measurements (σ = 0.0) and using three circles with radius r = 1.0 and center at (−3.5, 4.0), (0, −2.0), and (3.5, 4.0) as the initial guesses, the estimated shape of cavities by using the SDM is shown in Fig. 12 after 15 iterations. It can be seen from this figure that the scheme obtains a reliable estimation of $f_1(x, y)$, $f_2(x, y)$, and $f_3(x, y)$, except for the center region, and the CPU time (on a 586-60 MHz personal computer) used in the SDM is about 35 s. The reason for inaccurate estimation near the center region of the domain is the same as in numerical test case 2, because no temperature readings were obtained within this region.

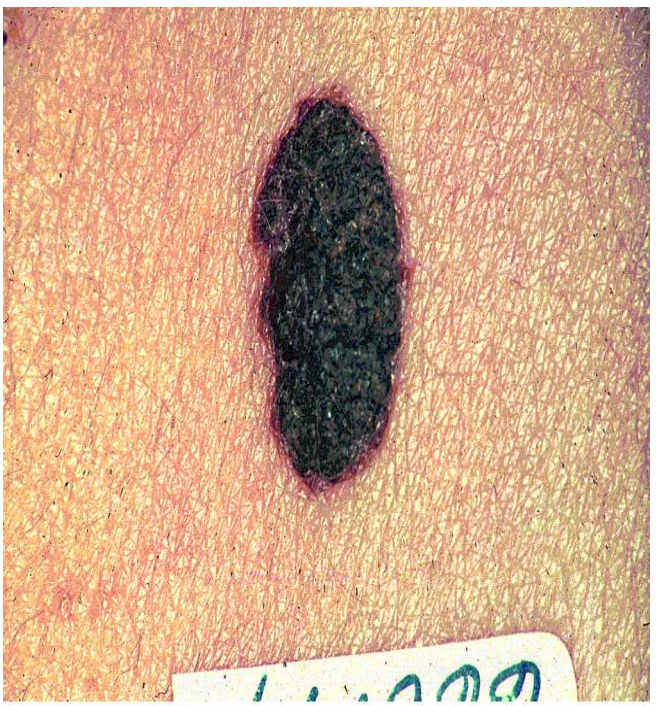

(D)

Fig. 12 Exact and estimated cavities when using s = 0.0 and M = 40 in test case 3.

(E)

Fig. 13 Exact and estimated cavities when using s = 0.4 and M = 40 in test case 3.

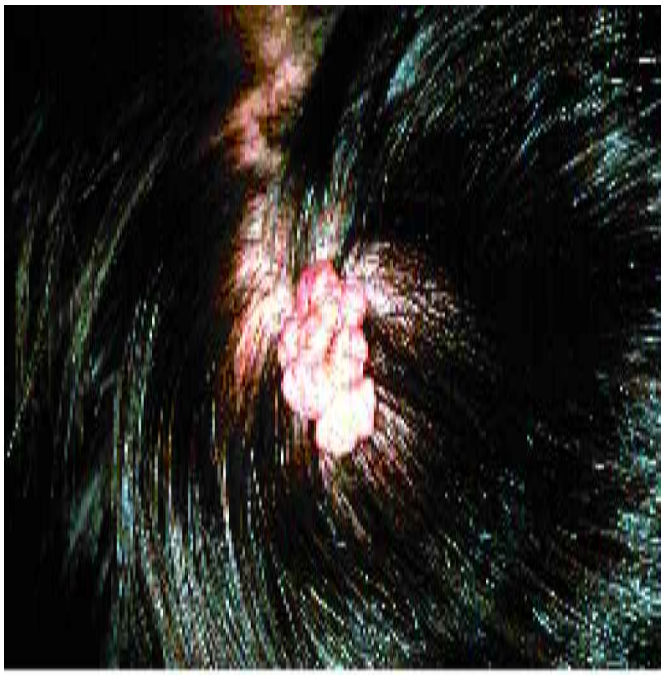

Fig. 14 Exact and estimated cavities when using s = 0.9 and M = 40 in test case 3.

Next, when the standard deviation of the measurement errors with $\sigma = 0.4$ and 0.9 are assumed, the simulated inexact measurement temperature can be obtained from Eq. (16). Here, $\sigma = 0.4$ and 0.9 represent about 4 and 9% measurement error, respectively, because the average measured temperature is about 10. The inverse solution can be obtained after 6 (20 s CPU time) and 3 (11 s CPU time) iterations for $\sigma = 0.4$ and 0.9, respectively. The estimated cavities for these two cases are shown in Figs. 13 and 14. From Figs. 12–14, we conclude again that when the measurement errors are considered, the SDM performs well in this inverse geometry problem in estimating the unknown shape of cavities.

From the preceding three numerical test cases, we learned that the SDM in estimating unknown multiple cavities does not need any assumptions such as the cubic spline fitting used in Ref. 9. When unknown cavities have some sharp corners, such as the shape used in case 1, the SDM can still be applied to obtain good estimation, but a cubic spline APG algorithm may not perform well because cubic spline fitting cannot produce any sharp corners.

X. Conclusions

The SDM together with the BEM were successfully applied for the solution of the inverse problem to determine the unknown irregular cavities configuration by utilizing temperature readings. Several test cases involving different shape, location, and number of cavities were examined, and the measurement errors were also considered. The results show that the SDM does not require accurate initial guesses of the unknown quantities, does not need any extra assumptions such as a cubic spline fitting, needs a very short CPU time on a 586-60 MHz personal computer, estimates the multiple unknown cavities easily, and is not sensitive to the measurement errors when performing the inverse calculations.

Acknowledgment

This work was supported in part through the National Science Council, Republic of China, Grant NSC-87-2212-E-006-107.

References

[1]Huang, C. H., and Ozisik, M. N., "Inverse Problem of Determining Unknown Wall Heat Flux in Laminar Flow Through a Parallel Plate Duct," *Numerical Heat Transfer*, Vol. 21, No. 1, Pt. A, 1992, pp. 55–70.

[2]Tervola, P., "A Method to Determine the Thermal Conductivity from Measured Temperature Profiles," *International Journal of Heat and Mass Transfer*, Vol. 32, No. 8, 1989, pp. 1425–1430.

[3]Huang, C. H., and Ozisik, M. N., "Optimal Regularization Method to Determine the Unknown Strength of a Surface Heat Source," *International Journal of Heat and Fluid Flow*, Vol. 12, No. 2, 1991, pp. 173–178.

[4]Huang, C. H., and Ju, T. M., "An Inverse Problem of Simultaneously Estimating Contact Conductance and Heat Transfer Coefficient of Exhaust Gases Between Engine's Exhaust Value and Seat," *International Journal of Numerical Methods in Engineering*, Vol. 38, No. 5, 1995, pp. 735–754.

[5]Hsieh, C. K., and Su, K. C., "A Methodology of Predicting Cavity Geometry Based on the Scanned Surface Temperature Data-Prescribed Surface Temperature at the Cavity Side," *Journal of Heat Transfer*, Vol. 102, No. 2, 1980, pp. 324–329.

[6]Hsieh, C. K., and Kassab, A. J., "A General Method for the Solution of Inverse Heat Conduction Problems with Partially Specified System Geometries," *International Journal of Heat and Mass Transfer*, Vol. 29, No. 1, 1986, pp. 47–58.

[7]Kassab, A. J., and Hsieh, C. K., "Application of Infrared Scanners and Inverse Heat Conduction Methods to Infrared Computerized Axial Tomography," *Review of Scientific Instruments*, Vol. 58, No. 1, 1987, pp. 89–95.

[8]Hsieh, C. K., Choi, C. Y., and Liu, K. M., "A Domain Extension Method for Quantitative Detection of Cavities by Infrared Scanning," *Journal Nondestructive Evaluation*, Vol. 8, No. 2, 1989, pp. 195–211.

[9]Kassab, A. J., and Pollard, J., "A Cubic Spline Anchored Grid Pattern Algorithm for High Resolution Detection of Subsurface Cavities by the IR-CAT Method," *Numerical Heat Transfer*, Vol. 26, No. 1, Pt. B, 1994, pp. 63–78.

[10]Beck, J. V., Blackwell, B., and St. Clairi, C. R., *Inverse Heat Conduction . . . . . Ill-Posed Problem*, Wiley, New York, 1985.

[11]Huang, C. H., and Chao, B. H., "An Inverse Geometry Problem in Identifying Irregular Boundary Configurations," *International Journal of Heat and Mass Transfer*, Vol. 40, No. 9, 1997, pp. 2045–2053.

[12]Brebbia, C. A., and Dominguez, J., *Boundary Elements: An Introductory Course*, McGraw–Hill, New York, 1989.

[13]Alifanov, O. M., "Solution of an Inverse Problem of Heat Conduction by Iteration Methods," *Journal of Engineering Physics*, Vol. 26, No. 4, 1972, pp. 471–476.

[14]*IMSL Library Edition 10.0, User's Manual: Math Library Version 1.0*, International Mathematical and Statistical Library, Houston, TX, 1987.